FLUORINATED NANOCARBONS AS CATHODE IN PRIMARY LITHIUM BATTERIES

Wei Zhang, LMI, CLERMONT-FERRAND II University, Aubière, 63177, FRANCE
Axel Houdayer, LMI, CLERMONT-FERRAND II University, Aubière, 63177, FRANCE
Katia Guérin, LMI, CLERMONT-FERRAND II University, Aubière, 63177, FRANCE
Marc Dubois, LMI, CLERMONT-FERRAND II University, Aubière, 63177, FRANCE
André Hamwi, LMI, CLERMONT-FERRAND II University, Aubière, 63177, FRANC
Rachid Yazami, CALTECH-CNRS, ILMEE, Pasadena, CA 91125, USA

Keywords
Intercalation, carbon fluorides, primary lithium battery

ABSTRACT

The electrochemical performances of fluorinated carbon nanofibres have been tested for a use as cathode material in primary lithium battery using $LiBF_4$ PC:DME 1M as electrolyte. For a very narrow fluorination range [420-450°C], the fluorine content in the carbon nanofibres increases up to $CF_{0.78}$ and so do both the energy and the power densities. A maximum of 8057 $W.kg^{-1}$ power density has been reached. Moreover, a current density of 6C can be used for such fluorinated carbon nanofibres. Such high electrochemical values can be correlated to the amount of unfluorinated carbon located in the core of the carbon nanofibres. Owing to solid state ^{13}C NMR which can accurately evaluated this fraction, a minimum of 10% of unfluorinated carbon nanofibre is necessary in order to insure a good conducting behaviour.

INTRODUCTION

Lithium primary batteries are commonly used for many applications such as cameras, electrical lock, electronic counter, electronic measurement equipment, emergency power source, memory back-up, military and implantable medical devices. These applications require power sources with high energy densities, good reliability, safety and long life. One of the attractive chemistries is that provided with a fluorine based cathode and more particularly carbon fluoride (CFx). In fact in the Li/CFx battery system, a high oxidation-reduction potential of the cathode reaction is combined with low gravimetric density of light C and F elements. The use of CFx materials as the active cathode material in primary lithium batteries was first demonstrated by Watanabe et al. (Watanabe, 1972) and then a few years later, the first Li/CF_1 batteries were commercialised by Matsushita Electric Co. in Japan (Fukuda, 1975). Commercial Li/CF_x batteries use a coke based cathode having a F:C molar ratio equal or slightly higher than unity. The most important features of the Li/CF_1 batteries are: high energy density (up to 560 $Wh.kg^{-1}$), high average operating voltage (around 2.4 V vs. Li^+/Li), long shelf life (> 10 years at room temperature), stable operation and wide operating temperatures (-40°C – 170°C). However due to kinetic limitations associated with the poor electrical conductivity of strongly covalent CF_1 material, the battery can sustain only low to medium range discharge currents. In order to develop such batteries for new application such as for space long term exploratory missions, the range of achievable discharge currents should be extended, so as to increase the power density. To address this issue, our approach consisted of setting the kinetics conditions for carbon fluorination aimed at increasing the intrinsic electrical conductivity of CF_x cathode materials.

EXPERIMENTAL

Synthesis: High purity (> 90%) Carbon Nanofibres (CNFs) which are 8-20 mm in diameter with 2-20 micron lengths have been furnished by MER corporation, they have been obtained by CVD method and then post-treated under argon atmosphere at 1800°C. Fluorinated carbon nanofibres ($CNFT_T$) were prepared with 200 mg of CNFs at temperatures T_T ranging between 380°C and 480°C in F2 atmosphere for a reaction time of 16h. The fluorination level has been calculated by quantitative ^{19}F NMR (Chamssedine, 2007).

Physico-chemical characterizations: NMR experiments were performed with Bruker Avance spectrometers, with working frequency for ^{13}C of 73.4 MHz. Two NMR Bruker probes were used: a static and a special Cross Polarization/Magic Angle Spinning probe with fluorine decoupling on a 4 mm rotor. The ^{19}F-^{13}C match was optimised on polytetrafluoroethylene (PTFE); the ^{19}F Π/2 pulse width was 4 μs. For MAS spectra, a

simple sequence (t-acquisition) was used with a single π/2 pulse length of 3.5 μs for ^{13}C. TEM images have been made on a FEI CM200 operating at 200 kV.

Electrochemical methods: For electrochemical tests, carbon nanofibres fluorides electrodes were composed of the sample $CNFT_T$ (about 75% by weight, w/w), acetylene black (15%, w/w) to insure electronic conductivity and polyvinylidene difluoride (PVDF, 10%, w/w) as binder. Dibutylphtalate (DBP) was then added (about 20% w/w) until the mixture becomes homogeneous and slightly viscous. The mixture was then poured on a PTFE container and allowed to dry at ambient temperature, then at 40°C for several hours. Discs were cut from the film, washed in methanol to remove DBP and dried in air at ambient temperature in vacuum at 80°C for several hours. The about 1.2 cm in diameter cathode discs are typically 13-17 mg in weight and about 100 μm in thickness. Coin cells were assembled in a dry box filled with argon and used a metallic lithium disc for the anode, a microporous polypropylene separator soaked with a 1 molar solution of $LiBF_4$ in PC:DME (1:1 vol.) electrolyte and the $CNFT_T$ based cathode. The 2016 coin cells were discharged at constant rates ranging between C/20 and 6C at room temperature.

RESULTS AND DISCUSSION

In order to increase the intrinsic electrical conductivity of CFx cathode materials, a better choice of the starting carbonaceous material, i.e. carbon nanofibres (CNFs) vs. coke combined with a minute control of the fluorination conditions, i.e. temperature T_T, fluorine gas flow rate (g/min) and time (Yazami, 2007) were made. This allowed fluorinated CNFs, CFx (noted hereafter $CNFT_T$) with targeted composition 'x' $0.2<x<\sim1.0$ to be achieved. A characteristic of this new family of CFx materials is the presence of nano-domains of unfluorinated carbon atoms that facilitate the electron flow within the particles.

Recently we showed that increasing the fluorination temperature T_T leads to a progressive fluorination which processes from the outer part of the $CNFT_T$ towards its core (Chamssedine, 2007). The physicochemical characteristics of the $CNFT_T$ samples have been extensively studied by complementary techniques (^{19}F, ^{13}C solid state NMR, EPR, XRD, Raman spectroscopy and TEM). Four fluorination temperature zones can be distinguished [4]:

- i) For T_T lower than 420 °C, the fluorination rate 'x' assessed by both weight uptake and ^{19}F NMR is low: $0 < x < 0.2$. In particular, for T_T = 380 °C the composition is $CF_{0.04}$ whereas for graphite at the same reaction conditions CF0.60 is achieved. Only a surface fluorination of the CNFs occurred.
- ii) When T_T is in the 420-435 °C range, the F:C ratio is drastically increased: $0.31<x<0.70$. As shown by TEM (**Figure 1.**), fluorination progresses towards the internal walls when the temperature is increased. The structure of $CNFT_T$ consists in $(C_2F)_n$ type carbon fluoride ('stage-2' compound with FCCF slabs stacking sequence) of the fluorinated part located near the surface and unfluorinated CNF core. Concomitantly, Raman spectroscopy measurements confirmed the progressive increase of the structural disordering in the carbon nanofibres with the fluorination.
- iii) Rising T_T to the 435-450 °C range resulted in $CNFT_T$ with a nearly constant x~0.7-0.8. Here the fluorination progressed toward the core without major structural changes of the fluorinated parts. Unfluorinated domains are still present as clearly evidenced by ^{13}C NMR analysis.
- iv) When T_T was set higher than 450°C, a jump in composition is observed up to 480°C, then the later reaches a value around x~1.0. Finally, at 490°C, a partial exfoliation occurs resulting in a partial decomposition of the fluorinated carbon nanofibres towards the conversion of $(C_2F)_n$-type graphite fluoride into $(CF)_n$- type one ('stage-1' compound with FCF slabs stacking sequence).

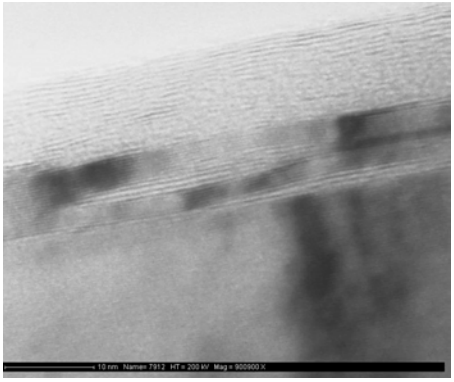

Figure 1. TEM bright field images of $CNFT_T$ for F:C = 0.21.

Accordingly, for 450 < T_T < 480°C, the fluorinated domains, which are the electrochemically active part of the cathode material as the source of the high energy density, are intermixed at nano-scale with unfluorinated domains. The later play a key role in enhanced intrinsic electrical conductivity of the $CNFT_T$ materials.

Pursuing our earlier physical-chemical characterization work on various fluorinated nanofibres, the electrochemical performances in primary lithium battery have been investigated. The galvanostatic rate capability profiles of samples synthesized at different temperature are detailed in Fig. 2. Only a few studies have covered the electrochemical properties of fluorinated nanocarbons (Hamwi, 1998; Touhara, 2002). However, carbon fluorides have been intensively studied as cathode materials in high energy densities lithium batteries (Hagiwara, 1988; Watanabe, 1980; Yazami, 1995). The discharge profiles of the Li/ $CNFT_T$ cells exhibit a characteristic plateau corresponding to the formation of LiF owing to the equation:

$$(CF_x)_n + nx\ Li^+ + nx\ e^- \rightarrow n\ C + nx\ LiF.$$

The discharge profiles of $CNFT_T$ differ greatly in shape according to the composition. This result is mainly due to the increase of F:C molar ratios with T_T leading to higher discharge capacity.

For T_T lower than 420°C (x< 0.2), no discharge potential plateau is observed (**Figure 2a.**), even at a C/20 rate. This can be related to the fluorine fixation site. As a matter of fact, as F is expected to be located at the surface of the fluorinated CNF, the concentric form of the sheets results in a slight dispersion of the C-F bonding energy and the different electrochemical potentials of LiF formation lead to a gradual discharge plateau. Moreover, as the fluorination temperature range is narrow, the non-dependence of the C-F bonding with reaction temperature is easily understandable. For the other samples, at low discharge current density, the average discharge potential is set in a very narrow range (2.45- 2.6V) (**Figure 2b-2d.**). This quasi stability is in agreement with the covalent C-F bonding which does not change upon fluorination as showed by a ^{19}F and ^{13}C NMR study (Chamssedine, 2007). In fact for samples with 0.59<x<0.82, the fluorination temperature range is narrow, therefore the C-F bonding energy is expected not to vary much in this range, leading to a narrow discharge voltage window at low discharge rates.

Although the discharge voltage and the fluorine content of $CNFT_T$ are close to those reported in $(C_2F)_n$-type graphite fluoride, the achieved discharge capacity of the $CNFT_T$ materials synthesized between 428 and 450°C is about 30% higher than those of $(C_2F)_n$ (Touhara, 1982). **Figure 3.** depicts the Ragone plots (energy vs. power density) of tested cathodes, including commercial CF_1 material for comparison. Note that squared root scale has been used for the power density axis for convenience. **Table 1.** summarizes the theoretical capacity, the maximum achieved discharge rate, the energy density and the power density. Under nC-rate the discharge current is set so as the theoretical capacity is reached after 1/n hours. Hence at 2C- and C/2- rates the cathode discharge is expected to take 0.5 hour and 2 hours, respectively.

Figure 2. shows both the discharge capacity and the energy density increased with the F:C compositional ratio. An impressive 8057 $W.kg^{-1}$ power density associated with a high 1749 $Wh.kg^{-1}$ energy density were achieved in $CNFT_T$ with F:C = 0.76 as shown in **Table 1**. Here, the power density is 6 times higher than the one of commercial graphite fluorides. Then, for F:C > 0.80, the maximum power density decreases but is still higher than the one of commercial graphite fluorides. So, CF_x treated between 435 and 450°C having a fluorination level between 0.7 and 0.82 yield better electrochemical performances in $CNFT_T$ series. The faradic yield, which is defined as the ratio of the achieved discharge capacity and the theoretical specific discharge one, is here an increasing function of 'x'. In fact under low discharge rates it varied from 74% in $CF_{0.21}$ and 93% in $CF_{0.76}$ to nearly 100% in $CF_{0.82}$. This particular behavior may be related to the fluorine induced disorder of the $CNFT_T$ biphasic structure. Since the $CNFT_T$ cathode reduction is limited by the lithium ions diffusion within the multi-tubes structure, lower temperature fluorination preserves better the parent tubular layers structure and generates only a few damages. Therefore, the lithium diffusion is hindered by a low defects density. As the fluorination temperature T_T increases, additional intercalated fluorine creates more strains for their accommodation, which leads to increased defects density. The latter include cracks in the carbon layers, opening of the nanofibres ends and crystal lattice distortion. Such defects are additional and easy paths for lithium ions diffusion within the core of the fluorinated structure and access the electrochemically active C-F sites. Moreover, the presence of the non-fluorinated carbons in the $CNFT_T$ core even in small amounts favors higher electron flow and accordingly enhances the electrode reaction kinetics. In fact the effect of enhanced conductivity is more pronounced at higher discharge rates were the power density difference with the state of the art CF_1 becomes obvious. As can be seen in **Figure 2**. whatever the $CNFT_T$ cathode material, including a lightly fluorinated $CF_{0.21}$, both the achieved C-rate and power density are higher than for CF_1.

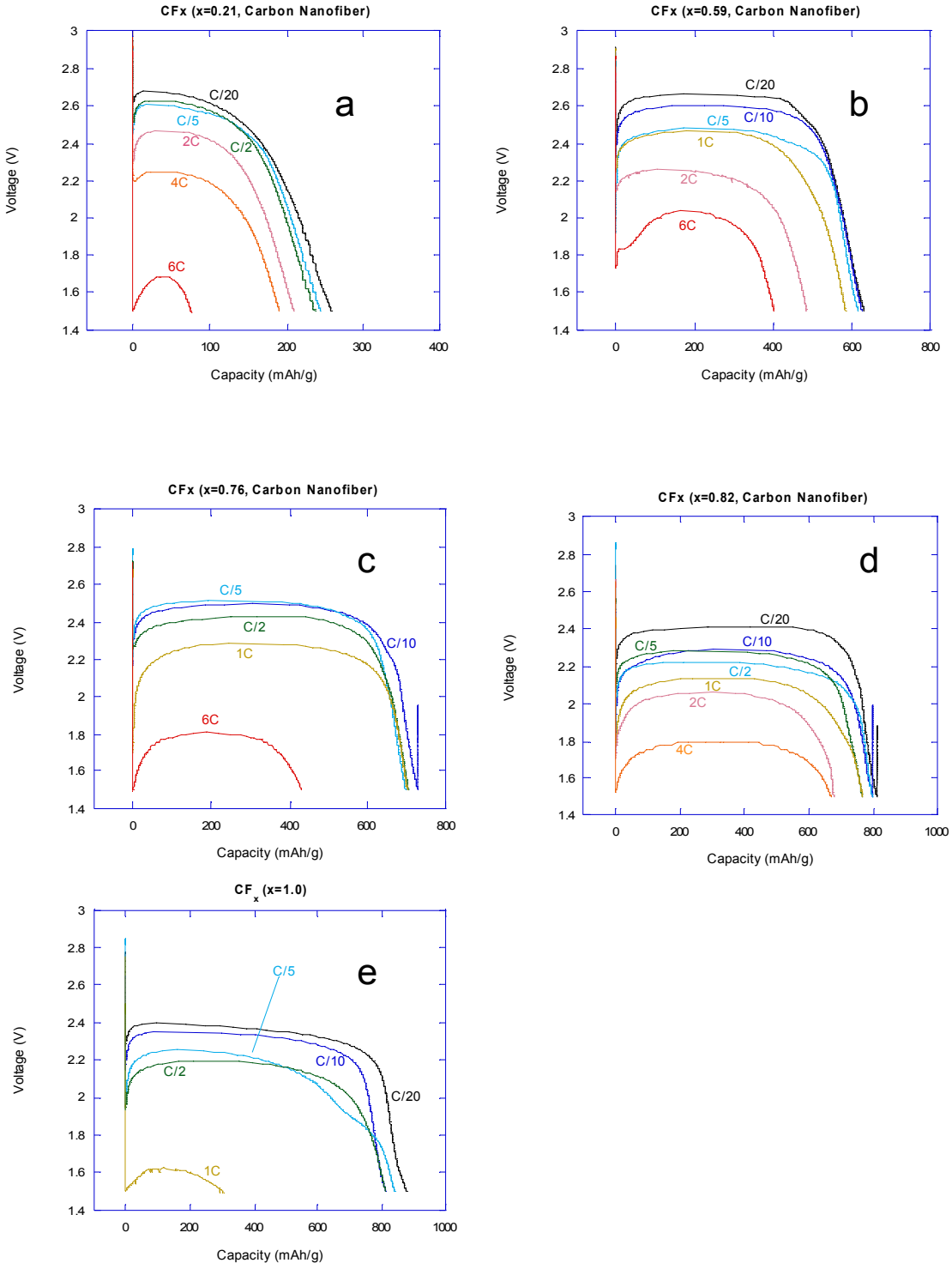

Figure 2. Galvanostatic discharge curves for different current densities of $CNFT_T$ for F:C = 0.21 (a), F:C = 0.59 (b), F:C = 0.76 (c) and F:C = 0.82 (d) compared to the ones of commercial $(CF)_n$ with F:C = 1 (e).

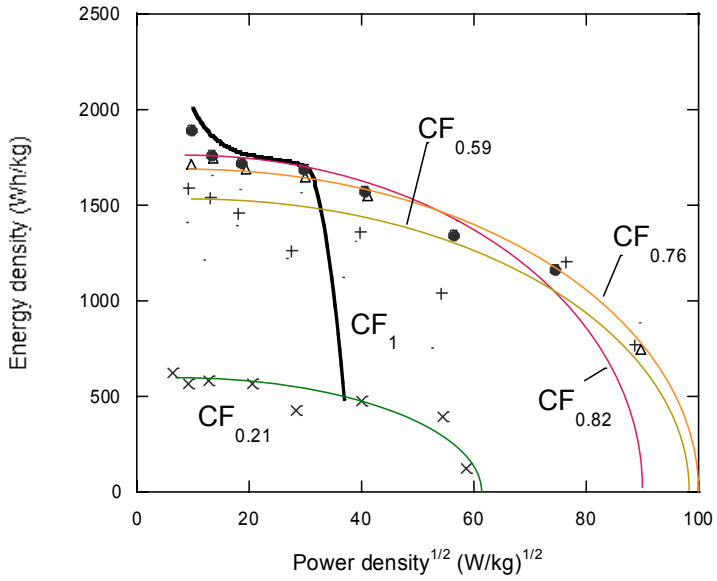

Figure 3. Ragone plot of $CNFT_T$ and commercial CF_1 cathodes.

Table 1.
Electrochemical performances of some fluorinated carbon nanofibres compared with the ones of commercial graphite fluoride

CFx		Theoretical capacity (mAh/g)	Max. C-rate available	Max. Energy density (Wh/kg)	Max. Power density (W/kg)
Commercial CFx (x=1.0)		865	1C	2012	1370
Carbon Nanofiber	0.21	352	**6C**	620	3434
	0.59	681	**6C**	1587	7866
	0.76	771	**6C**	1749	8057
	0.82	797	4C	1897	5564

In order to quantify the minimum fluorinated part quantity needed to insure a good electrical conductivity, a complementary study by ^{13}C NMR has been performed. ^{13}C-NMR gives additional information about the nature of the interaction between carbon and fluorine atoms, i.e. the C-F bonding, and the presence of non-fluorinated carbon atoms. For F:C > 0.32, two resonance lines are present at 84-88 and 42 ppm/TMS, both related to carbon atoms exhibiting sp^3 hybridization. The first line (with area denoted $S_{C\text{-}F}$) is assigned to carbon atoms covalently bonded to fluorine atom as expected for the fluorination performed in this range of temperatures (Panich, 1999). The other peak is related to non-fluorinated sp^3 carbons atoms (area S_{Csp3}) as in the case of $(C_2F)_n$ (Dubois, 2006). This line is a solid proof of the $(C_2F)_n$ formation. The third large resonance peak centered near 120 ppm is mainly assigned to non-fluorinated sp^2 carbon atoms but also to carbon atoms in weak interaction with fluorine (~140 ppm) (Dubois, 2004), their respective area are denoted $S_{Cgraphitic}$ and $S_{C\text{---}F}$.

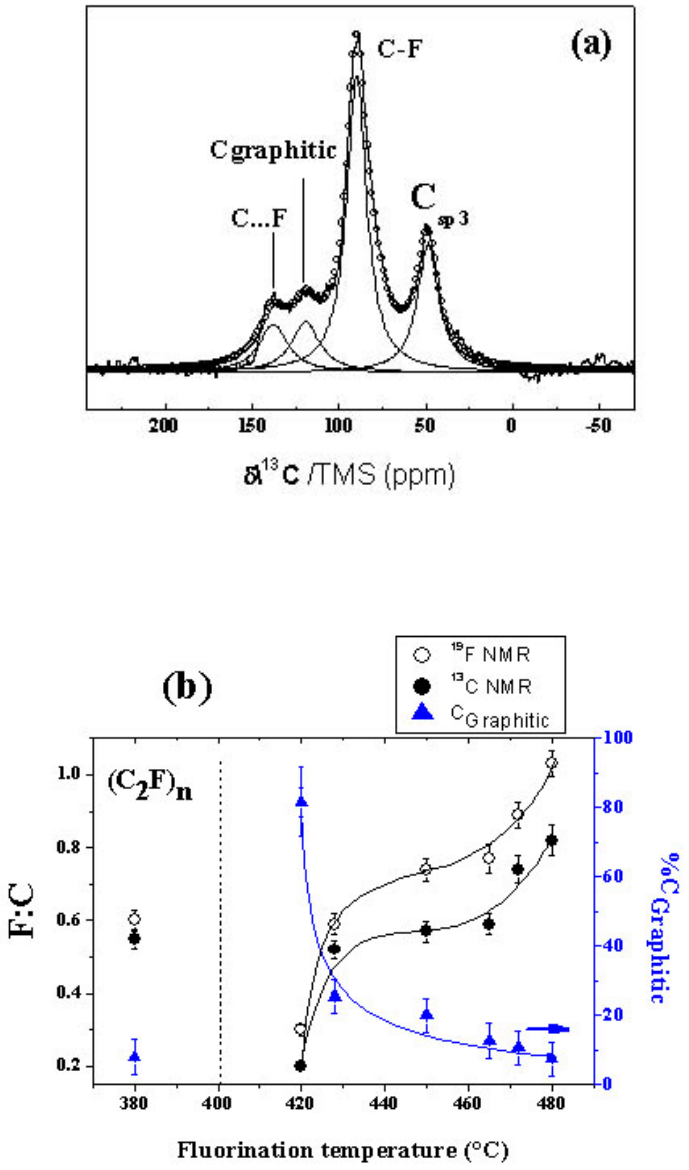

Figure 4 a. ^{13}C MAS NMR spectrum of CNF472 (10 kHz spinning rate), b. Evolution of F:C ratio as seen by ^{19}F (o) and ^{13}C (●) NMR.
The fraction of graphitic carbons is also reported (▲). For comparison, data concerning $(C_2F)_n$ type graphite fluoride are added.

First, it must be noticed that the area ratio of the two sp^3 carbon resonances is nearly constant regardless of the fluorine content; we have $S_{C\text{-}F}$ / S_{Csp3} = 2.43, 2.37 and 2.34 for CNF fluorinated at 428, 465 and 472 °C. For comparison, on the spectrum of $(C_2F)_n$ graphite fluoride, the $S_{C\text{-}F}/S_{Csp3}$ ratio is close to 1.5. This sample was obtained by fluorination of graphite at 380 °C and exhibits a F:C ratio of 0.60. If λ designs the fraction of graphitic carbon atoms, it can be estimated by the $S_{Cgraphitic}/S_{tot}$ ratio (S_{tot} is the sum of the area i.e. $S_{C\text{---}F}$ + $S_{Cgraphitic}$ + $S_{C\text{-}F}$ + S_{Csp3}). In the graphite derived $CF_{0.60}$ sample, F:C (as seen by ^{13}C NMR) is equal to 0.55 and λ= 0.08. For x<1, due to the underestimation of the carbon atoms bonded to fluorine, λ is slightly higher than the real value. The F:C ratio can be estimated by ^{13}C MAS NMR by the ratio [$S_{C\text{---}F}$ + $S_{C\text{-}F}$] /S_{tot}. As T_T increases, the fluorine content 'x' increases and concomitantly, the fraction λ gradually decreases**. Figure 4b.** shows similar general evolution for the ratio estimated by ^{19}F and ^{13}C NMR. However, the F:C ratio, as seen by ^{13}C NMR, is systematically underestimated by a factor of 1.3. Nevertheless, λ can be used as an indicator of the progress of the fluorination reaction. Lower the λ value, larger the fluorination domains. For λ lower than 10%, the maximum power density available decreases. 10% of residual parent CNF appears as the low end threshold limit in order for the cathode to sustain a high discharge drain. This limit is low indicating that small amounts of unfluorinated carbons allow the electrochemical performances to be improved. On the other hand, the increase in 'x' goes without significant structural modification up to T_T = 450 °C. The formed C-F bonds are basically covalent.

CONCLUSIONS

High current densities (6C) and high power density (>8000 $W.kg^{-1}$) are now achievable owing to fluorinated carbon nanofibres, treated under pure fluorine gas at temperatures ranged between 435 and 450°C, are used as cathode in primary lithium batteries. A controlled fluorination of CNFs results in a material where fluorinated and unfluorinated domains co-exist at the nanometer scale. The unfluorinated regions into the core should act as an easy electron transport path within the graphite fluoride structure and decrease the ohmic drop which can be correlated to the strong electron localization for strong C-F bonding energy. The minimum amount of unfluorinated carbons have been accurately determined by solid state ^{13}C NMR; 10% of residual graphitic carbons contributes to enhance the electrical conductivity in fluorinated carbon nanofibres and therefore reduces cathode polarization under high rates.

ACKNOWLEDGMENTS

The authors thank MER Corporation, Tucson, AZ, for generously providing the CNFs and D. A. Ivanov, from Institut de chimie des surfaces et interfaces de Mulhouse, France, for TEM images and valuable discussions concerning this work.

REFERENCES

Chamssedine, F., Dubois M., Guérin K., Giraudet, J., Masin, F., Ivanov, D.A., Vidal, L., Yazami, R., Hamwi, A., (2007). Reactivity of Carbon Nanofibres with fluorine gas, *Chem. Mater.*, 19, [2], 161-172.

Dubois, M., Guérin, K., Pinheiro, J.P., Fawal, Z., Masin, F., Hamwi, A., (2004). NMR and EPR studies of room temperature highly fluorinated heat-treated under fluorine atmosphere, *Carbon*, 42, [10], 1931-1940.

Dubois, M., Giraudet, J., Guérin, K., Hamwi, A., Fawal, Z., Pirotte, P., Masin, F. (2006). EPR and Solid-State NMR : Studies of Poly(dicarbon monofluoride) $(C_2F)_n$, *J. Phys. Chem. B*, 110, 11800 - 11808.

Fukuda, M., Iijima, T., (1975). *in: D. H. Collins (Ed.) : Power Sources 5*, ACADEMIC PRESS, 713.

Hagiwara, R., Lerner, M., Bartlett, N., Nakajima, T., (1988). A lithium/carbon fluoride (C_2F) primary battery, *J. Electrochem. Soc.,* [135], 2393 - 2394.

Hamwi, A., Gendraud, P., Gaucher, H., Bonnamy, S., Béguin, F., (1998). Electrochemical properties of carbon nanotube fluorides in a lithium cell system, *Mol. Cryst. Liq. Cryst.*, [310], 185 - 190.

Panich, A.M., (1999). Nuclear magnetic resonance study of fluorine-graphite intercalation compounds and graphite fluorides, *Synth. Metals,* [100], 169-185.

Touhara, H., Fujimoto, H., Tressaud, A., Watanabe, N., (1982). On the discharge reaction mechanism in graphite fluoride-lithium batteries, *J. Fluorine Chem.*, [21], 27.

Touhara, H., Inahara, J., Mizuno, T., Yokoyama, Y., Okanao, S., Yanagiuch, K., Mukopadhyay, I., Kawasaki, S., Okino, F., Shirai, H., Xu, W. H., Kyotani, T., Tonita, A., (2002). Property control of new forms of carbon materials by fluorination, *J. Fluorine Chem.,* [114], 181 - 188.

Watanabe, N., Fukuda, M., (1970). US Patent 3 536 532, and (1972). 3 700 502.

Watanabe, N., (1980). Two types of graphite fluorides, $(CF)_n$ and $(C_2F)_n$, and discharge characteristics and mechanisms of electrodes of $(CF)_n$ and $(C_2F)_n$ in lithium batteries, *Solid State Ionics* [1] 87-110.

Yazami R., (1995). *in: T. Nakajima (Ed.), Chemistry, Physics and Applications of Fluorine-Graphite and Fluoride -Carbon Compounds*, Marcel Dekker Inc., 251.

Yazami, R., Hamwi, A., (2007). Subfluorinated graphite fluorides as electrode materials, *US Patent Serial No. 11/560,570, patent pending*.